DOI: 10.1002/chem.200903587

Efficient Photoinduced Energy Transfer Mediated by Aromatic Homoconjugated Bridges

José Osío Barcina,*[a] Noelia Herrero-García,[a] Fabio Cucinotta,[b] Luisa De Cola,[b] Pablo Contreras-Carballada,[c] Rene M. Williams,*[c] and Andrés Guerrero-Martínez*[b]

Dedicated to Professor Antonio García Martínez on occasion of his retirement

Abstract: A new donor–bridge–acceptor (D-B-A) dyad consisting of ruthenium(II) and iridium(III) species separated by an homoconjugated bridge derived from 7,7-diphenylnorbornane [Ir-Nor-Ru]$^{3+}$ has been synthesised. The photophysical and electrochemical properties of the heterodinuclear complex have been compared with those of the analogous homodinuclear complexes [Ru-Nor-Ru]$^{4+}$ and [Ir-Nor-Ir]$^{2+}$. Transient absorption spectra on the nanosecond and sub-picosecond timescales show, for the first time, that an homoconjugated bridge can mediate efficiently in the photoinduced energy transfer from the iridium(III) to the ruthenium(II) centres according to a Dexter-type mechanism.

Keywords: energy transfer · homoconjugation · iridium · photochemistry · ruthenium

Introduction

The design of supramolecular multicomponent systems for photoinduced energy/electron transfer is an important field of research with applications in the development of electroluminescent displays, molecular-scale devices and solar-energy conversion systems.[1] In donor–bridge–acceptor (D-B-A) dyads, not only the chromophores, but also the bridge plays a fundamental role in mediating the energy-transfer process and the search for bridges with molecular wire behaviour still remains a challenge.[2] The electronic coupling between donor and acceptor, which is a main determining factor for the (Dexter) energy/electron transfer processes, can be provided by various types of electronic interactions that are inherent to the intervening medium between donor and acceptor. Whereas much attention is focused on π-conjugated bridges,[2,3] σ-conjugation (through a σ-bond interaction),[4] cross-conjugated pathways,[5] helical bridges (through foldamer coupling),[6] π-stacked systems[7] and hexaarylbenzenes with toroidal delocalisation[8] are also modes for electronic communication that can be very effective (compared with through (vacuum) space separation). Next to σ, π, spiro,[9] toroidal and cross-conjugation (Scheme 1), an unexplored area for D-B-A systems is provided by aromatic homoconjugation. Homoconjugation can be defined as the orbital overlap of two π systems separated by a non-conjugat-

[a] Prof. Dr. J. Osío Barcina, N. Herrero-García
Departamento de Química Orgánica, Facultad de Ciencias Químicas
Universidad Complutense de Madrid
Ciudad Universitaria s/n, 28040 Madrid (Spain)
Fax: : (+34) 91-3944103
E-mail: josio@quim.ucm.es

[b] F. Cucinotta, Prof. Dr. L. De Cola, Dr. A. Guerrero-Martínez
Physikalisches Institut, Westfälische Wilhelms-Universität
Mendelstrasse 7, 48149 Münster (Germany)
Fax: (+49) 251-980-2834
E-mail: aguerrero@uvigo.es

[c] Dr. P. Contreras-Carballada, Dr. R. M. Williams
Photonics Group, HIMS, Universiteit van Amsterdam
Nieuwe Achtergracht 129, 1018 WS Amsterdam (The Netherlands)
Fax: (+31) 20-525-6456
E-mail: R.M.Williams@uva.nl

Supporting information for this article is available on the WWW under http://dx.doi.org/10.1002/chem.200903587.

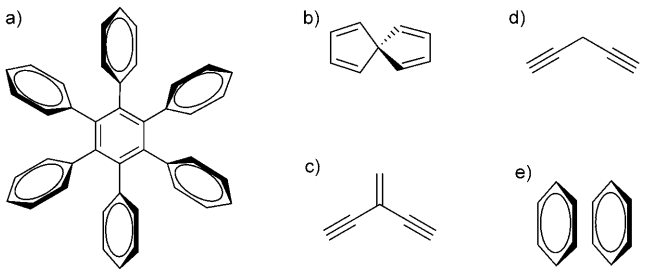

Scheme 1. Examples of systems showing a) toroidal conjugation, b) spiro-conjugation, c) cross-conjugation, d) homoconjugation and e) π stacking.

ed group, such as CH_2 (IUPAC).[10] Homoconjugative interactions between double and triple bonds have been extensively studied. Electron delocalisation in homoconjugated alkenes is well established in the case of cationic homoaromatic compounds in which the positive charge is the driving force for delocalisation.[10e,f] However, the situation in neutral homoconjugated molecules remains controversial, even in the case of homoaromatic compounds.[10a–f,h] Surprisingly, homoconjugative interactions between aromatic rings have received less attention. In that respect, it has been argued that in diphenylmethane, the simplest candidate for aromatic homoconjugated compounds, the saturated methylene group should act as a barrier to conduction.[11] Diphenylmethane can be described as a free rotator, the most stable conformation of which is the helical disposition, thus avoiding homoconjugative interactions between the aromatic rings.[12] This situation can be modified by forcing the aryl rings to adopt a cofacial conformation as we have found in the case of 7,7-diphenylnorbornane (DPN) (**1**) (Scheme 2).[12,13] We have shown that in oligomers and polymers derived from **1**, aromatic homoconjugation contributes to the electron delocalisation along the backbone structure.[13a–c] These results show that the delocalisation mediated by aromatic homoconjugation is more effective than in homoconjugated acetylenes, in which no significant homoconjugative stabilisation is observed.[10a,b]

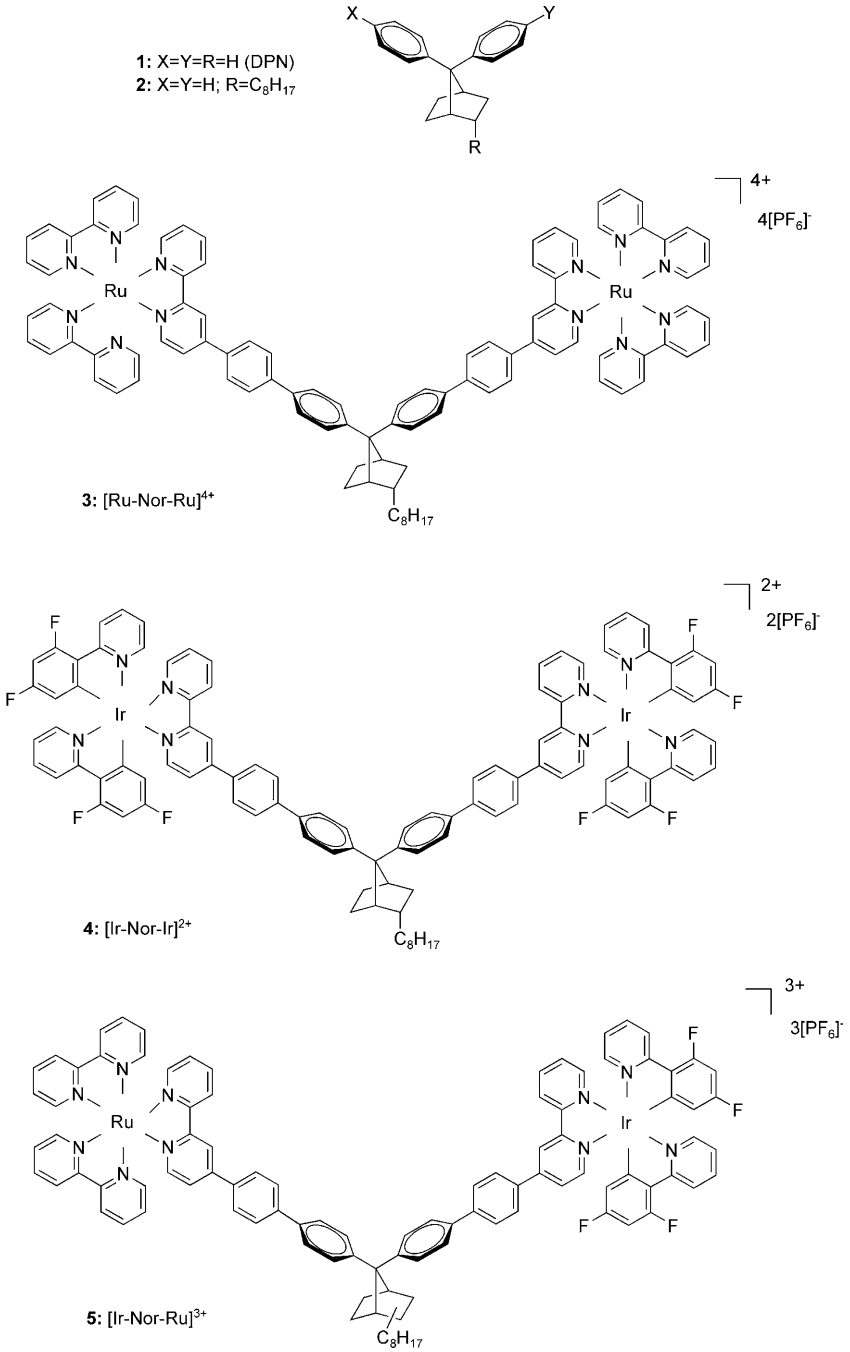

Scheme 2. Structures of **1** and complexes **3**, **4** and **5**.

To gain further understanding of the role played by the bridging unit, we report now the synthesis and photophysical properties of the first example of a D-B-A dyad with aromatic homoconjugated bridge **5** as well as its homodinuclear analogues **3** and **4** (Scheme 2).

Results and Discussion

As chromophores for this study, we have chosen complexes containing Ru^{II}[14] and Ir^{III}[15] species due to the effective molecular wire behaviour that has been observed in dinuclear Ir^{III}/Ru^{II} complexes with conjugated *p*-phenylene bridges.[16] Iridium complexes forming part of supramolecules for the monitoring of energy- and electron-transfer processes have been widely studied, and the literature presents several examples of interesting wire-like molecules based on bis-terpyridine linear geometries.[15] Additionally, iridium metal

complexes are being extensively studied for the potential and very promising application in electroluminescent devices thanks to their high photostability and emission tunability.[17] The synthesis of compounds **3**, **4** and **5** (Scheme 2) has been carried out by following the methodology described previously for the preparation of **1** derivatives and Ir^{III}/Ru^{II} complexes (Scheme 3). Alkyl chain (C_8H_{17}) is introduced in the norbornane skeleton (**2**) to increase the solubility of the derivatives during the synthetic route.

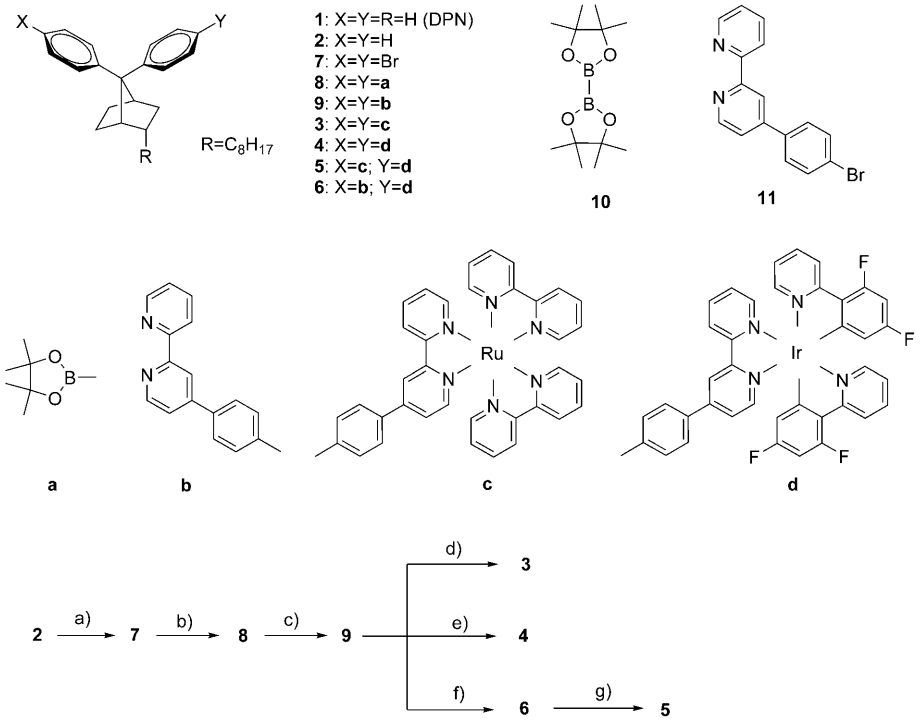

Scheme 3. a) Br_2 (88%); b) **10**/[Pd(dppf)Cl_2] (dppf = 1.1′-bis(diphenylphosphino)ferrocene)/KAcO/DMSO (87%); c) **11**/[Pd(PPh_3)$_4$]/Na_2CO_3/toluene/H_2O (54%); d) [Ru(bpy)$_2Cl_2$]/1,2-dimethoxyethane (DME)/ethylene glycol (2:1)/ultrasound (85%); e) [{Ir(ppyFF)$_2$(μ-Cl)}$_2$]/ethylene glycol/$CHCl_3$ (3:1) (66%); f) [{Ir(ppyFF)$_2$(μ-Cl)}$_2$]/ethylene glycol/$CHCl_3$ (3:1) (51%); g) [Ru(bpy)$_2Cl_2$]/ethylene glycol/$CHCl_3$ (3:1)/ultrasound (62%).

Photophysical properties

Absorption and emission spectroscopy: The absorption spectra of the homodinuclear complexes [Ir-Nor-Ir]$^{2+}$ and [Ru-Nor-Ru]$^{4+}$, and the heterodinuclear compound [Ir-Nor-Ru]$^{3+}$ in diluted (optical density <0.1), air-equilibrated acetonitrile at 293 K closely resemble the sum of the individual spectra of the mononuclear units [Ir(ppyFF)$_2$(bpy)]$^+$ (ppyFF = 2-(2,4-difluorophenyl)pyridine, bpy = 2,2′-bipyridine) and [Ru(bpy)$_3$]$^{2+}$ (see Figure 1). The spectrum of [Ir-Nor-Ru]$^{3+}$ shows both absorption bands of the two homodinuclear species. The intense peaks at 246 and 288 nm can be assigned to spin-allowed ligand-centred (^{1}LC) transitions involving the ppyFF and the peripheral bpy groups,[18,19] together with transitions associated with the preferred cofacial disposition of the aryl ring in **1**.[13]

Moreover, the broad band centred at around 326 nm can be assigned to spin-allowed π–π* transitions localised on **1**-substituted bridging bipyridines,[16a] which includes the weaker spin-allowed Ir-based metal–ligand charge-transfer (MLCT) transitions, as also observed for [Ir-Nor-Ir]$^{2+}$.[18,20] Additionally, in the visible region (400–550 nm) we can find the typical spin-allowed Ru-based MLCT absorption band,[14] which is half as intense as that observed for the [Ru-Nor-Ru]$^{4+}$ complex.

To quantify possible energy-transfer processes after excitation of the energy-donor component (see below), we have to consider that no selective excitation on the iridium MLCT band is possible, due to the full overlap in the absorption bands of the two ruthenium and iridium homodinuclear species (Figure 1). However, the dinuclear complexes spectra show an isoabsorptive point at about 332 nm, in which the Ir and Ru moieties absorb the same fraction of incident light. Figure 2a shows the emission spectra of [Ir-Nor-Ir]$^{2+}$, [Ir-Nor-Ru]$^{3+}$, [Ru-Nor-Ru]$^{4+}$, and the reference compound [Ir(ppyFF)$_2$(bpy)]$^+$, recorded upon excitation at 332 nm at room temperature from dilute solutions in acetonitrile (optical density <0.1).

The luminescence spectrum of the homodinuclear complex [Ir-Nor-Ir]$^{2+}$ exhibits an emis-

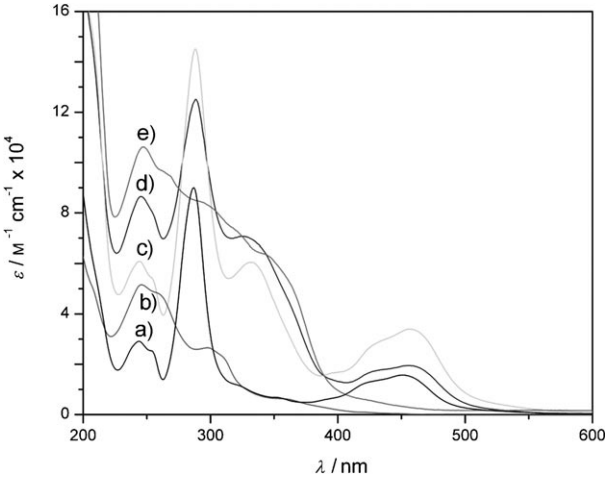

Figure 1. Absorption spectra of [Ru(bpy)$_3$]$^{2+}$ (a), [Ir(ppyFF)$_2$(bpy)]$^+$ (b), [Ru-Nor-Ru]$^{4+}$ (c), [Ir-Nor-Ru]$^{3+}$ (d) and [Ir-Nor-Ir]$^{2+}$ (e) in dilute acetonitrile solution at 298 K.

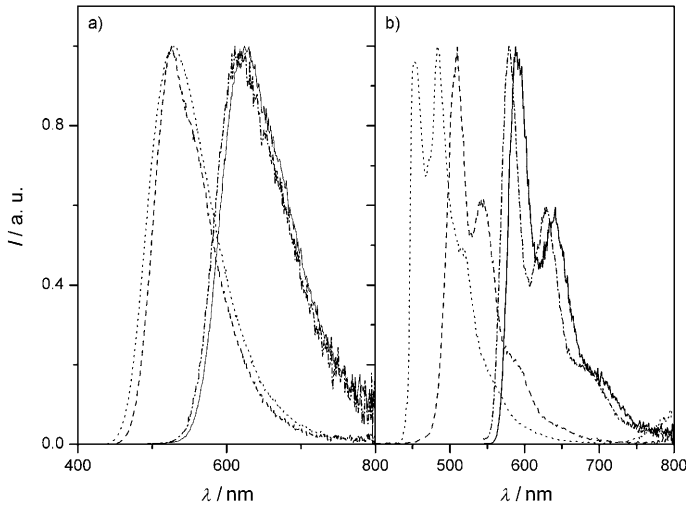

Figure 2. Emission spectra of $[Ir(ppyFF)_2(bpy)]^+$ (•••••), $[Ir\text{-}Nor\text{-}Ir]^{2+}$ (-----), $[Ru\text{-}Nor\text{-}Ru]^{4+}$ (–•–•) and $[Ir\text{-}Nor\text{-}Ru]^{3+}$ (——) in a) a dilute solution in acetonitrile at 298 K, and b) a butyronitrile rigid matrix at 77 K ($\lambda_{exc}=332$ nm).

sion centred at 526 nm, which originates from a state with mixed ^{3}MLCT–^{3}LC character, mostly located on the bipyridine ligand, as for the parent compound $[Ir(ppyFF)_2(bpy)]^+$.[15a] It is noteworthy that $[Ir\text{-}Nor\text{-}Ir]^{2+}$ complex shows a 20 nm blueshifted emission, when compared with similar homodinuclear iridium complexes with fully extended π conjugation,[16a] since the presence of an sp^3 carbon, bearing **1**, diminishes the conjugation in the bridge between the two iridium centres, thus causing a rise in the LUMO orbital energy.[13a] The homodinuclear complex $[Ru\text{-}Nor\text{-}Ru]^{4+}$ displays an emission band centred at 625 nm, slightly redshifted relative to $[Ru(bpy)_3]^{2+}$,[14] due to the larger conjugation on one of the bipyridines, that lowers its LUMO level and consequently the energy of the ^{3}MLCT transition.[16a] Keeping the excitation wavelength at 332 nm, we have recorded the luminescence spectrum of the heterodinuclear complex $[Ir\text{-}Nor\text{-}Ru]^{3+}$, which shows complete quenching of the iridium-based emission, and a broad band centred at 625 nm, as observed for $[Ru\text{-}Nor\text{-}Ru]^{4+}$ complex. No significant difference in the Ru-based emission intensities are observed for $[Ir\text{-}Nor\text{-}Ru]^{3+}$ and $[Ru\text{-}Nor\text{-}Ru]^{4+}$ after excitation at 332 nm, which implies very efficient energy transfer (see Table 1 and below).

In Figure 2b the low-temperature emission spectra under dilute conditions are shown, reflecting the same trend observed at room temperature. Both $[Ir\text{-}Nor\text{-}Ir]^{2+}$ and $[Ru\text{-}Nor\text{-}Ru]^{4+}$ exhibit structured emission profiles, with maxima at 508 and 580 nm, respectively; the first emission band is 18 nm blueshifted when compared with the room temperature emission, while the Ru-based homodinuclear complex shows a larger hypsochromic shift of 45 nm. This behaviour matches the statement of a mixed ^{3}LC–^{3}MLCT state for the $[Ir\text{-}Nor\text{-}Ir]^{2+}$ emission, which in a rigid matrix, due to the strong destabilisation of the ^{3}MLCT state, is predominantly a ligand-centred emission, whereas the $[Ru\text{-}Nor\text{-}Ru]^{4+}$ emission retains its ^{3}MLCT character.[21] The emission spectrum of the heterodinuclear $[Ir\text{-}Nor\text{-}Ru]^{3+}$ complex is essentially identical to that of $[Ru\text{-}Nor\text{-}Ru]^{4+}$ compound, even at this low temperature, showing again complete intramolecular quenching of the iridium unit emission.

All the photophysical data related to the emission spectra of the complexes are listed in Table 1, including the emission quantum yields and the time-resolved measurements. The lifetimes of the Ru-based emission in the heterodimetallic complex at room temperature and in the frozen matrix are very similar to those of $[Ru(bpy)_3]^{2+}$ and $[Ru\text{-}Nor\text{-}Ru]^{4+}$,[14] which shows analogous excited states. However, the marked lifetime differences of the iridium-centred emission at 77 K in the case of $[Ir\text{-}Nor\text{-}Ir]^{2+}$ and the iridium parent compound $[Ir(ppyFF)_2(bpy)]^+$, has been ascribed to a low-energy, long-lived emission due to a ^{3}LC state localised on the homoconjugated bridge unit of iridium homodinuclear complexes,[16a] which at low temperature becomes the lowest excited state. Electrochemical characterisations were performed by cyclic voltammetry in 10^{-3} M solutions in acetonitrile, containing 0.1 M tBu_4NPF_6 as the supporting electrolyte, the results of which led to the observation of characteristic electrochemical features of iridium and ruthenium complexes (see the Supporting Information).[14,22]

Transient absorption spectroscopy: The nanosecond transient absorption spectra of $[Ir(ppyFF)_2(bpy)]^+$, $[Ir\text{-}Nor\text{-}Ir]^{2+}$ and $[Ir\text{-}Nor\text{-}Ru]^{3+}$ were recorded upon excitation at 330 nm at room temperature in deaerated acetonitrile (Figure 3). The transient absorption spectra of the dinuclear iridium complex register a long-lived broad absorption, stretching from 400 to 820 nm (Figure 3a), which arises from several contributions, such as the bpy radical anion and the ligand-centred triplet state. The absence of such long-lived transient absorption bands in deaerated solutions of $[Ir(ppyFF)_2(bpy)]^+$ (Figure 3b) indicates the formation of the excited state of the bpy-oligophenylene–**1** ligand for **4**. In the case of the $[Ir\text{-}Nor\text{-}Ru]^{3+}$ complex, the transient spectra (Figure 3c) exhibit two features in the region from

Table 1. Photophysical data.

	298 K[a]					77 K[b]			
	Ir^{III}		Ru^{II}			Ir^{III}		Ru^{II}	
	λ_{max} [nm]	τ [ns][d]	λ_{max} [nm]	τ [ns][d]	$10^2\times\phi$	λ_{max} [nm]	τ [μs][d]	λ_{max} [nm]	τ [μs][d]
$[Ir\text{-}Nor\text{-}Ir]^{2+}$	526	150	–	–	1.8	508	37.0	–	–
$[Ru\text{-}Nor\text{-}Ru]^{4+}$	–	–	625	197	7.4	–	–	593	5.9
$[Ir\text{-}Nor\text{-}Ru]^{3+}$	–	[c]	625	200	7.4	[c]	–	590	5.8
$[Ir(ppyFF)_2(bpy)]^+$	529	140	–	–	2.2	484	4.4	–	–
$[Ru(bpy)_3]^{2+}$	–	–	619	156	6.2	–	–	579	5.7

[a] In aerated acetonitrile, $\lambda_{exc}=332$ nm. [b] In a butyronitrile rigid matrix, $\lambda_{exc}=332$ nm. [c] Too low in intensity to be detected accurately by [d]. [d] Time-correlated single-photon counting method.

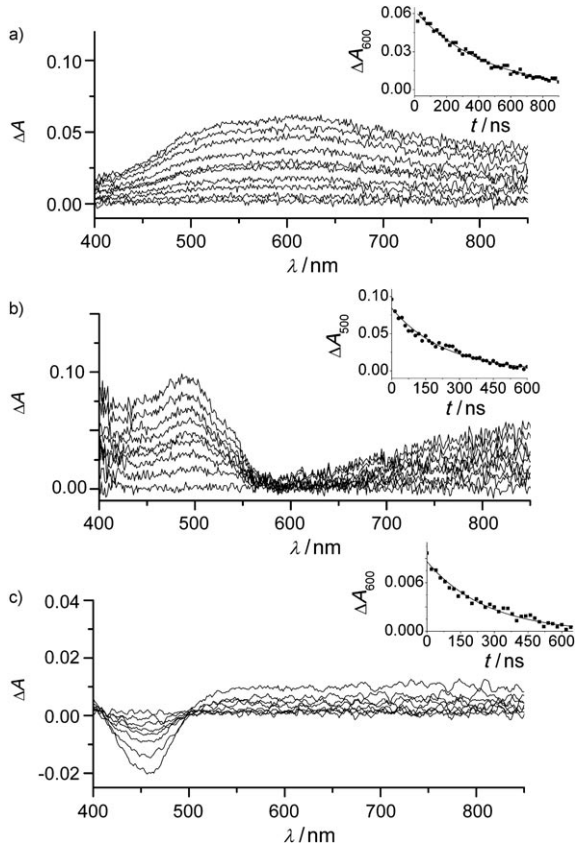

Figure 3. Transient absorption spectra and decay kinetics of a) [Ir-Nor-Ir]$^{2+}$, b) [Ir(ppyFF)2(bpy)]$^{+}$ and c) [Ir-Nor-Ru]$^{3+}$ in acetonitrile at 293 K (λ_{exc} = 332 nm, < 5 mJ pulse^{-1}, 2 ns half-width at half maximum, FWHM). The insets show the decay at 600 nm for a) and c), and at 500 nm for b).

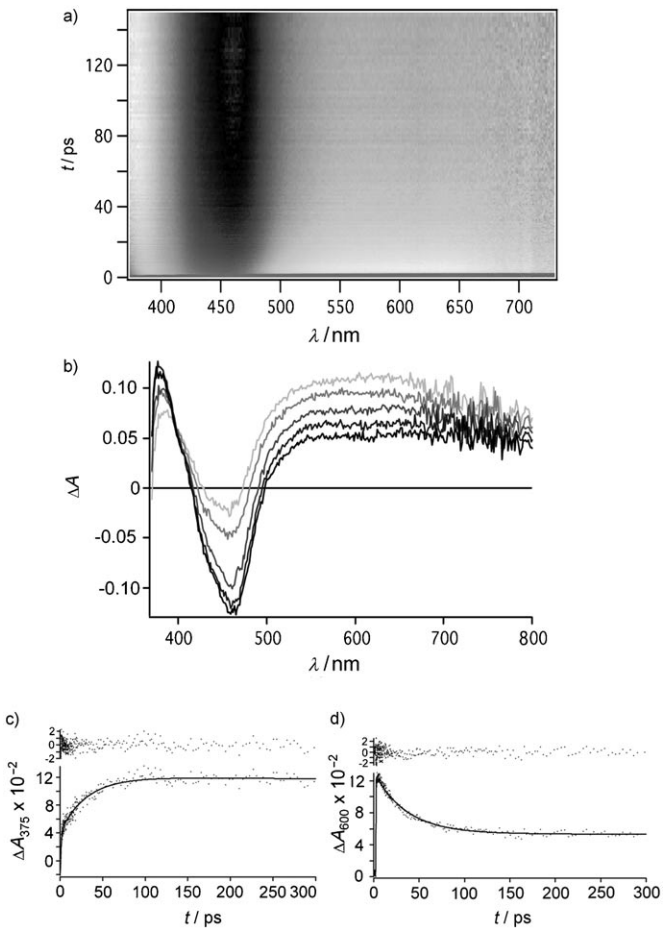

Figure 4. a) Sub-picosecond transient absorption data matrix of [Ir-Nor-Ru]$^{3+}$ in acetonitrile (λ_{exc} = 370 nm, 130 fs FWHM). Dark grey is negative, light grey is positive b) Overlay of several sub-picosecond absorption spectra at different time delays. Kinetics profiles at c) 375 and d) at 600 nm.

400–850 nm. The negative absorption at 460 nm is related to the bleaching of the ruthenium-centred ground state, whereas no bands attributed to the iridium component are observed. The broad feature in the region from 500–850 nm is assigned to the formation of the radical anion of the bpy-oligophenylene–**1** ligand. All bands decay monoexponentially with lifetimes slightly longer than those registered by time-resolved emission measurements, due to the existence of possible underlying long-lived absorbing species that modifies the evolution at the selected wavelengths.

Since it was not possible to monitor the energy-transfer processes on the nanosecond timescale for the iridium–ruthenium mixed metal complexes,[16a] sub-picosecond transient absorption spectroscopy was performed. Figure 4a shows the femtosecond transient absorption data matrix obtained for an solution of the [Ir-Nor-Ru]$^{3+}$ complex in acetonitrile after laser excitation at 370 nm;[23] several processes can be observed. Positive transient absorptions are shown in light grey shades, while negative bands are represented by dark grey. After laser excitation, a broad band is formed between 500 and 800 nm, corresponding to the iridium-centred excited state, which decays abruptly within the first 150 ps of the measurement. Concomitantly with this decay, two new bands appear: a positive absorption below 400 nm, ascribed to the reduced bipyridine radical anion on the ruthenium moiety and a negative transient absorption, located between 400 and 500 nm, which originates from the bleaching of the ruthenium-centred ground state. As the process evolves, this state is depleted, while the ^{3}MLCT excited state is formed, and the band becomes more negative over time.

By overlaying transient absorption spectra at different time delays we obtain Figure 4b. For comparison, the sub-picosecond transient absorption spectra of the two homodinuclear complexes were also recorded (see the Supporting Information), showing characteristic features for these types of systems.[20,24] The analysis of the kinetics of the energy-transfer process in the [Ir-Nor-Ru]$^{3+}$ system was obtained from the band evolution at 375 nm, which shows that complete quenching of the iridium-centred excited state takes place within the first 150 ps of the measurement (Figure 4c). A reasonable complementarity is observed in Figure 4d, which shows a decay of the signal at 600 nm as time proceeds. We ascribe this fast component to energy transfer occurring from the higher-lying iridium triplet state to the lower-lying ruthenium triplet state. The energy-transfer rate

has been calculated from $k_{ET}=1/\tau-1/\tau_0$, in which τ_0 is the iridium lifetime given by the time-resolved emission measurements, and τ is the quenched lifetime obtained from kinetic analysis (30.9 ps). A global fit procedure using TIMP was applied to the data matrix,[25] evaluating all ≈300 kinetic traces, resulting in an energy-transfer rate of $k_{ET}=3.24\times10^{10}\,s^{-1}$. Taking into account an unquenched lifetime of 150 ns (see Table 1) and a quenched lifetime of 30.9 ps, an energy-transfer efficiency of 99.98% has been calculated ($\eta=1\text{-}\tau_q/\tau_{ref}$).

Although there are several examples based on iridium/ruthenium and ruthenium/osmium bimetallic complexes interconnected by linear polyphenylene conjugated spacers,[2,16a] no examples of energy-transfer processes in organometallic-based homoconjugated systems have been reported, to the best of our knowledge. Thus, a reasonable comparison between these fully extended π-conjugated complexes and the homoconjugated [Ir-Nor-Ru]$^{3+}$ compound, in terms of the k_{ET} dependence with the intermetallic distance, can be made. Regarding the estimated Ir–Nor(C7)–Ru distance and the energy-transfer rate between the metal units (29.7 Å, $3.24\times10^{10}\,s^{-1}$), an intermediate behaviour is observed with respect to previously reported binuclear complexes bearing a bridge consisting of four phenylene groups, such as [Ir-ph$_4$-Ru]$^{3+}$ (28.3 Å, $3.6\times10^{11}\,s^{-1}$),[16a] in which energy transfer proceeds by a clear Dexter mechanism.[26] Even though the observed energy-transfer process for the [Ir-Nor-Ru]$^{3+}$ compound is slower than in [Ir-ph$_4$-Ru]$^{3+}$, due to the higher energy of the triplet state localised on the homoconjugated spacer, the rate of this process is fast in relation to other fully extended π-conjugated species.[24] Within a Dexter-type energy-transfer mechanism (double electron transfer), several bridge-related aspects are of key importance. The mixing of donor and acceptor orbitals with the bridge orbitals, which is governed by symmetry and the energy gap, is essential,[2,3,4] since electronic coupling is required. As such the donor–bridge coupling is rather combination specific and comparison with different donor chromophores is less useful. It should be noted that electron delocalisation in aromatic homoconjugated systems is less effective than in conjugated compounds,[13] and therefore, the energy band gap is higher for homoconjugated bridges.[13a] This result indicates that the energy transfer takes place according to a Dexter-type mechanism, which formally consists of a double electron exchange between donor excited state and acceptor.[27]

Conclusion

The photophysical behaviour of [Ir-Nor-Ru]$^{3+}$ demonstrates that energy transfer between donor/acceptor components through aromatic homoconjugation is an effective mechanism, and could be used for vectorial energy and electron transport over very long distances (e.g., 3 nm). This is the first example reported to date of effective photoinduced energy transfer mediated by aromatic homoconjugated bridges and provides a new tool to tune the properties of D-B-A systems by changing the structural features of the bridging unit. Work is currently in progress in our laboratories to design novel D-B-A systems with aromatic homoconjugated bridges and to study the possibility of molecular wire behaviour in these complexes.

Experimental Section

Spectroscopy and photophysics: UV/Vis absorption spectra were recorded on a Varian Cary 5000 double-beam UV/Vis-NIR spectrophotometer; all spectra were measured from quartz cuvettes (1 cm, Hellma). Steady-state emission spectra in the spectral range of 300–800 nm were recorded on a HORIBA Jobin–Yvon IBH FL-322 Fluorolog 3 spectrometer equipped with a 450 W Xenon arc lamp, double grating excitation and emission monochromators (2.1 nm mm^{-1} dispersion; 1200 grooves mm^{-1}) and a Hamamatsu R928 photomultiplier tube or a TBX-4-X single-photon-counting detector. Emission and excitation spectra were corrected for source intensity (lamp and grating) and emission spectral response (detector and grating) by standard correction curves.

Time-resolved measurements up to ≈5 μs were performed by using the time-correlated single-photon counting (TCSPC) option on the Fluorolog 3 instrument. A NanoLED (402 nm; FWHM < 750 ps) with repetition rates between 10 kHz and 1 MHz was used to excite the sample. The excitation source was mounted directly on the sample chamber at 90° to a double-grating emission monochromator (2.1 nm mm^{-1} dispersion; 1200 grooves mm^{-1}) and collected by a TBX-4-X single-photon-counting detector. Signals were collected by using an IBH DataStation Hub photon counting module and data analysis was performed using the commercially available DAS6 software (HORIBA Jobin Yvon IBH).

For excited-state lifetimes >10 μs, a different experimental setup was used, by equipping the Fluorolog 3 with the FL-1040 phosphorescence module with a 70 W xenon flash tube (FWHM = 3 ms) with a variable flash rate (0.05–25 Hz). The signals were recorded on the TBX-4-X single-photon-counting detector and collected with a multichannel scaling (MCS) card in the IBH DataStation Hub photon-counting module and data analysis was performed as described above.

Emission quantum yields were determined with a Hamamatsu Photonics absolute PL quantum yield measurement system (C9920-02, equipped with a L9799-01 CW Xenon light source (150 W), monochromator, C7473 photonic multi-channel analyser, integrating sphere and employing U6039-05 PLQY measurement software (Hamamatsu Photonics, Ltd., Shizuoka, Japan).

Nanosecond transient absorption spectra were obtained by irradiating the samples (optical density ≈0.5) with 2 ns pulses (435 nm line, 5 mJ pulse^{-1}) of a tunable (420–710 nm) Coherent Infinity XPO laser. Lifetimes were determined using 1) a Coherent Infinity XPO laser (2 ns pulses FWHM) and a Hamamatsu C5680-21 streak camera equipped with a Hamamatsu M5677 low-speed single-sweep unit, 2) a sub-nanosecond single-photon counting setup with an excitation source that consists of a frequency doubled (300–340 nm, 1 ps, 3.8 MHz) output of a cavity dumped DCM dye laser (Coherent model 700) that was pumped by a mode-locked Ar-ion laser (Coherent 486 AS Mode Locker, Coherent Innova 200 laser).

Femtosecond transient absorption experiments were performed with a Spectra-Physics Hurricane titanium:sapphire regenerative amplifier system.[23] The full spectrum setup was based on an optical parametric amplifier (Spectra-Physics OPA 800C) as the pump. The residual fundamental light, from the pump OPA, was used for white-light generation, which was detected with a CCD spectrograph (Ocean Optics PC2000+ slave) for Vis detection. The polarisation of the pump light was controlled by a Berek Polarization Compensator (New Focus). The Berek Polarizer was always included in the setup to provide the magic-angle conditions. The probe light was double-passed over a delay line (Physik Instrumente, M-531DD) that provides an experimental time window of

3.6 ns with a maximal resolution of 0.6 fs step^{-1}. The OPA was used to generate excitation pulses at 370 nm. The laser output was typically 3.5–5 μJ pulse^{-1} (130 fs FWHM) with a repetition rate of 1 kHz. The samples were placed into cells of 2 mm path length (Hellma) and were stirred with a downward projected PTFE shaft, using a direct drive spectro-stir (SPECTRO-CELL). This stir system was also used for the white light generation in a 2 mm water cell.

Electrochemistry: Electrochemistry was performed with an Autolab Potentiostat in a three-electrode single-compartment cell. Ferrocene and tetrabutylammoniumhexafluorophosphate ($TBAPF_6$) were purchased from Sigma Aldrich. Electrolyte: 0.1 M $TBAPF_6$ in anhydrous acetonitrile (Sigma Aldrich), compound concentration was 10^{-3} M in the electrolyte. The cell was equipped with a platinum working electrode, a stainless steel counter electrode, and an Ag/AgCl pseudo-reference electrode.

See the Supporting Information for experimental details.

Compound 3: [Ru-Nor-Ru][PF_6]$_4$: 95.3 mg (86%); ^{1}H NMR (300 MHz, CD_3CN): δ = 8.88 (s, 2H), 8.81 (d, J = 8.3 Hz, 2H), 8.63 (dd, J = 8.0, 3.7 Hz, 8H), 8.24–8.12 (m, 10H), 8.06 (d, J = 8.3 Hz, 4H), 7.97–7.72 (m, 26H), 7.58–7.47 (m, 10H), 3.25–3.17 (m, 2H), 1.90–1.40 (m, 6H), 1.40–1.20 (m, 14H), 0.95–0.85 ppm (m, 4H); MS (ESI): m/z: 969.2 [$M^+ - 2PF_6$], 597.8 [$M^+ - 3PF_6$]; HRMS (ESI): m/z calcd for $C_{99}H_{88}N_{12}Ru_2$: 412.13354 [$M^+ - 4PF_6$]; found: 412.13378.

Compound 4: [Ir-Nor-Ir][PF_6]$_2$: 33.9 mg (42%); ^{1}H NMR (300 MHz, CD_3CN): δ = 8.79 (d, J = 1.5 Hz, 2H), 8.74 (d, J = 8.2 Hz, 2H), 8.35 (m, 4H), 8.20 (td, J = 7.9 and 1.4 Hz, 2H), 8.08–7.88 (m, 12H), 7.84–7.80 (m, 6H), 7.71–7.62 (m, 12H), 7.57 (t, J = 6.6 Hz, 2H), 7.10 (dd, J = 12.3, 6.1 Hz, 4H), 6.73 (t, J = 11.1 Hz, 4H), 5.77 (dd, J = 8.6 and 2.4 Hz), 3.27–3.16 (m, 2H), 1.90–1.35 (m, 6H), 1.35–1.20 (m, 14H), 0.94–0.82 ppm (m, 4H); MS (ESI): m/z: 2111.5 [$M^+ - PF_6$], 983.3 [$M^+ - 2PF_6$]; HRMS (ESI): m/z calcd for $C_{103}H_{80}N_8F_8Ir_2$: 983.28183 [$M^+ - 2PF_6$]; found: 983.28223.

Compound 5: [Ir-Nor-Ru][PF_6]$_3$: 74.2 mg (62%); ^{1}H NMR (300 MHz, CD_3CN): δ = 8.80 (s, 1H), 8.78 (s, 1H), 8.75 (d, J = 8.7 Hz, 1H), 8.71 (d, J = 8.1 Hz, 1H), 8.53 (dd, J = 8.0, 3.5 Hz, 4H), 8.36 (m, 2H), 8.21 (t, J = 7.9 Hz, 1H), 8.15–7.89 (m, 13H), 7.88–7.61 (m, 22H), 7.56 (t, J = 6.5 Hz, 1H), 7.49–7.38 (m, 5H), 7.13 (dd, J = 12.5, 6.4 Hz, 2H), 6.73 (t, J = 12.1 Hz, 2H), 5.78 (dd, J = 8.6, 2.4 Hz, 2H), 3.25–3.16 (m, 2H), 1.90–1.40 (m, 6H), 1.40–1.20 (m, 14H), 0.95–0.85 ppm (m, 4H); MS (ESI): m/z: 976.2 [$M^+ - 2PF_6$], 602.5 [$M^+ - 3PF_6$]; HRMS (ESI): m/z calcd for $C_{101}H_{84}N_{10}F_4RuIr$ [$M^+ - 3PF_6$]: 602.51631; found: 602.51664.

Acknowledgements

Financial support by the Spanish Ministerio de Educación y Ciencia (research project CTQ2007-67103-C02-01) is gratefully acknowledged.

[1] a) V. Balzani, F. Scandola, *Supramolecular Photochemistry*, Horwood, Chichester, **1993**; b) V. Balzani, A. Credi, M. Venturi, *Molecular Devices: Concepts and Perspectives for the Nanoworld*, Wiley-VCH, Weinheim, **2008**.

[2] "Molecular Wires. From design to Properties", thematic issue: *Top. Curr. Chem.* **2005**, *257*, 1–170, edited by L. de Cola.

[3] W. B. Davis, W. A. Svec, M. A. Ratner, M. R. Wasielewski, *Nature* **1998**, *396*, 60–63.

[4] a) R. M. Williams, M. Koeberg, J. M. Lawson, Y.-Z. An, Y. Rubin, M. N. Paddon-Row, J. W. Verhoeven, *J. Org. Chem.* **1996**, *61*, 5055–5062; b) H. Oevering, M. N. Paddon-Row, M. Heppener, A. M. Oliver, E. Cotsaris, J. W. Verhoeven, N. S. Hush, *J. Am. Chem. Soc.* **1987**, *109*, 3258–3269.

[5] a) B. C. van der Wiel, R. M. Williams, C. A. van Walree, *Org. Biomol. Chem.* **2004**, *2*, 3432–3433; for a review on cross-conjugation, see: b) M. Gholami, R. R. Tykwinski, *Chem. Rev.* **2006**, *106*, 4997–5027.

[6] M. Wolffs, N. Delsuc, D. Veldman, N. V. Anh, R. M. Williams, S. C. J. Meskers, R. A. J. Janssen, I. Huc, A. P. H. J. Schenning, *J. Am. Chem. Soc.* **2009**, *131*, 4819–4829.

[7] a) T. A. Zeidan, Q. Wang, T. Fiebig, F. D. Lewis, *J. Am. Chem. Soc.* **2007**, *129*, 9848–9849; b) M. Smeu, R. A. Wolkow, H. Guo, *J. Am. Chem. Soc.* **2009**, *131*, 11019–11029.

[8] a) C. Lambert, *Angew. Chem.* **2005**, *117*, 7503–7505; *Angew. Chem. Int. Ed.* **2005**, *44*, 7337–7339; b) S. V. Rosokha, I. S. Neretin, D. Sun, J. K. Kochi, *J. Am. Chem. Soc.* **2006**, *128*, 9394–9407.

[9] T. P. I. Saragi, T. Spehr, A. Siebert, T. Fuhrmann-Lieker, J. Salbeck, *Chem. Rev.* **2007**, *107*, 1011–1065.

[10] For a review on homoconjugated acetylenes, see: a) A. de Meijere, S. I. Kozhushkov, *Top. Curr. Chem.* **1999**, *201*, 1–42. See also: b) A. de Meijere, S. I. Kozhushkov, R. Boese, T. Haumann, D. S. Yufit, J. A. K. Howard, L. S. Khaikin, M. Traetteberg, *Eur. J. Org. Chem.* **2002**, 485–492; for recent studies on homobenzene, see: c) Z. Chen, H. Jiao, J. I. Wu, R. Herges, S. B. Zhang, P. von R. Schleyer, *J. Phys. Chem. A* **2008**, *112*, 10586–10594; d) F. Stahl, P. von R. Schleyer, H. Jiao, H. F. Schaefer III, K.-H. Chen, N. Allinger, *J. Org. Chem.* **2002**, *67*, 6599–6611; for a review on homoaromaticity, see: e) R. V. Williams, *Chem. Rev.* **2001**, *101*, 1185–1204. See also: f) C. Lepetit, B. Silvi, R. Chauvin, *J. Phys. Chem. A* **2003**, *107*, 464–473; for inorganic molecules with homoconjugation/homoaromaticity, see: g) Q. Zhang, S. Yue, X. Lu, Z. Chen, R. Huang, L. Zheng, P. von R. Schleyer, *J. Am. Chem. Soc.* **2009**, *131*, 9789–9799; stabilizing homoconjugative interactions between double and triple bonds are described in: h) R. Gleiter, R. Merger, H. Irngartinger, *J. Am. Chem. Soc.* **1992**, *114*, 8921–8932.

[11] a) D. K. James, J. M. Tour, *Top. Curr. Chem.* **2005**, *257*, 33–62; for examples of block copolymers with diphenylmethane subunits acting as conjugation interrupters, see: b) K.-Y. Peng, S.-A. Chen, W.-S. Fann, *J. Am. Chem. Soc.* **2001**, *123*, 11388–11397; c) P. G. Del Rosso, M. F. Almassio, S. S. Antollini, R. O. Garay, *Opt. Mater.* **2007**, *30*, 478–485; d) M. Beinhoff, L. D. Bozano, J. C. Scott, K. R. Carter, *Macromolecules* **2005**, *38*, 4147–4156; e) P. G. Del Rosso, M. F. Almassio, P. Aramendia, S. S. Antollini, R. O. Garay, *Eur. Polym. J.* **2007**, *43*, 2584–2593.

[12] "The Diphenylmethane Moiety": A. García Martínez, J. Osío Barcina in *Encyclopedia of Supramolecular Chemistry* (Eds.: J. L. Atwood, J. W. Steed), Marcel Dekker, New York, **2004**, pp. 452–456.

[13] a) J. Osío Barcina, M. R. Colorado Heras, M. Mba, R. Gómez Aspe, N. Herrero García, *J. Org. Chem.* **2009**, *74*, 7148–7156; b) N. Caraballo-Martínez, M. R. Colorado Heras, M. M. Blázquez, J. Osío Barcina, A. García Martínez, M. R. Torres Salvador, *Org. Lett.* **2007**, *9*, 2943–2946; c) A. García Martínez, J. Osío Barcina, A. de Fresno Cerezo, A.-D. Schlüter, J. Frahn, *Adv. Mater.* **1999**, *11*, 27–31; d) A. García Martínez, J. Osío Barcina, A. de Fresno Cerezo, R. Gutiérrez Rivas, *J. Am. Chem. Soc.* **1998**, *120*, 673–679.

[14] S. Campagna, F. Puntoriero, F. Nastasi, G. Bergamini, V. Balzani, *Top. Curr. Chem.* **2007**, *280*, 117–214.

[15] a) L. Flamigni, A. Barbieri, C. Sabataini, B. Ventura, F. Barigelletti, *Top. Curr. Chem.* **2007**, *281*, 143–203; b) L. Flamigni, J.-P. Collin, J.-P. Sauvage, *Acc. Chem. Res.* **2008**, *41*, 857–871.

[16] a) S. Welter, F. Lafolet, E. Cecchetto, F. Vergeer, L. De Cola, *ChemPhysChem* **2005**, *6*, 2417–2427. See also: b) M. Cavazzini, S. Quici, C. Scalera, F. Puntoriero, G. La Ganga, S. Campagna, *Inorg. Chem.* **2009**, *48*, 8578–8592; c) C. Sabatini, A. Barbieri, F. Barigelletti, K. J. Arm, J. A. G. Williams, *Photochem. Photobiol. Sci.* **2007**, *6*, 397–405; d) K. J. Arm, J. A. G. Williams, *Chem. Commun.* **2005**, 230–232; e) M. Cavazzini, P. Pastorelli, S. Quici, F. Loiseau, S. Campagna, *Chem. Commun.* **2005**, 5266–5268.

[17] For representative examples, see: a) A. B. Tamayo, S. Garon, T. Sajoto, P. I. Djurovich, I. M. Tsyba, R. Bau, M. E. Thompson, *Inorg. Chem.* **2005**, *44*, 87238732; b) W. J. Finkenzeller, M. E. Thompson, H. Yersin, *Chem. Phys. Lett.* **2007**, *444*, 273–279; c) J. Li, P. I. Djurovich, B. D. Alleyne, M. Yousufuddin, N. N. Ho, J. C. Thomas, J. C. Peters, R. Bau, M. E. Thompson, *Inorg. Chem.* **2005**, *44*, 1713–1727; d) A. Guerrero-Martínez, Y. Vida, D. Dominguez-Gutierrez, R. Q. Albuquerque, L. De Cola, *Inorg. Chem.* **2008**, *47*, 9131–9133.

[18] a) S. O. Garces, K. A. King, R. J. Watts, *Inorg. Chem.* **1988**, *27*, 3464–3471; b) K. Ichimura, T. Kobayashi, K. A. King, R. J. Watts, *J. Phys. Chem.* **1987**, *91*, 6104–6106.
[19] See, for example: K. Kalyanasundaram, *Photochemistry of Polypyridine and Porphyrin Complexes*, Academic Press, London, **1994**.
[20] F. Lafolet, S. Welter, Z. Popovic, L. De Cola, *J. Mater. Chem.* **2005**, *15*, 2820–2828.
[21] M. G. Colombo, A. Hauser, H. U. Güdel, *Inorg. Chem.* **1993**, *32*, 3088–3092.
[22] a) P. Coppo, E. A. Plummer, L. De Cola, *Chem. Commun.* **2004**, 1774–1775; b) A. B. Tamayo, B. D. Alleyne, P. I. Djurovich, S. Lamansky, I. Tsyba, N. N. Ho, R. Bau, M. E. Thompson, *J. Am. Chem. Soc.* **2003**, *125*, 7377–7387.
[23] For description and optical layout see the Supporting Information of: J. Baffreau, S. Leroy-Lhez, N. Van Anh, R. M. Williams, P. Hudhomme, *Chem. Eur. J.* **2008**, *14*, 4974–4992.
[24] a) J. K. McCusker, *Acc. Chem. Res.* **2003**, *36*, 876–887; b) S. Welter, N. Salluce, P. Belser, M. Groeneveld, L. De Cola, *Coord. Chem. Rev.* **2005**, *249*, 1360–1371.
[25] a) I. H. M. van Stokkum, D. S. Larsen, R. van Grondelle, *Biochim. Biophys. Acta Bioenerg.* **2004**, *1657*, 82–104; b) I. H. M. van Stokkum, R. H. Lozier, *J. Phys. Chem. B* **2002**, *106*, 3477–3485; c) Special issue: K. M. Mullen, I. H. M. van Stokkum, *J. Stat. Software* **2007**, *18*(3).
[26] F. Barigelletti, L. Flamigni, M. Guardigli, A. Juris, M. Beley, S. Chodorowski-Kimmes, J.-P. Collin, J.-P. Sauvage, *Inorg. Chem.* **1996**, *35*, 136–142.
[27] D. L. Dexter, *J. Chem. Phys.* **1953**, *21*, 836–850.

Received: December 31, 2009
Published online: April 13, 2010

